Energy Reports 8 (2022) 14658–14672

Contents lists available at ScienceDirect

Energy Reports

journal homepage: www.elsevier.com/locate/egyr

Research paper

A novel dynamic planning mechanism for allocating electric vehicle charging stations considering distributed generation and electronic units☆

Kayode E. Adetunji [a,*], Ivan W. Hofsajer [a], Adnan M. Abu-Mahfouz [b], Ling Cheng [a,*]

[a] School of Electrical and Information Engineering, University of the Witwatersrand, 1 Jan Smuts Avenue, Braamfontein, Johannesburg, 2000, South Africa

[b] Council for Scientific and Industrial Research (CSIR), Pretoria, 0184, South Africa

ARTICLE INFO

Article history:
Received 5 June 2022
Received in revised form 5 September 2022
Accepted 22 October 2022
Available online xxxx

Keywords:
Battery energy storage systems
Computational intelligence
Distributed generation
Electric vehicles
Electric vehicle charging station
Hybrid optimization algorithm
Planning mechanism
Reinforcement learning

ABSTRACT

Achieving a sustainable and efficient power systems network and decarbonized environment involves the optimal allocation of multiple distributed energy resource (DERs) unit types and flexible alternating current transmission systems (FACTS) to distribution networks. However, while the most focus is on optimization algorithms and multi-objective techniques, little to no attention is paid to the underlying mechanisms in planning frameworks. This paper goes beyond existing literature by investigating the impact of planning mechanisms in smart grid planning frameworks when considering the allocation of PV distributed generation units, battery energy storage systems, capacitor banks, and electric vehicle charging station facilities. First, a single- and multi-objective planning problem is formulated. Then, we propose a novel adaptive-dynamic planning mechanism that uses a recombination technique to find optimal allocation variables of multiple DER and FACTS types. To cope with the additional complexity resulting from the expanded solution space, we develop a hybrid stochastic optimizer, named cooperative spiral genetic algorithm with differential evolution (CoSGADE) optimization scheme, to produce optimal allocation solution variables. Through numerical simulations, it is seen that the proposed adaptive planning mechanism improves achieves a 12% and 14% improvement to the conventional sequential (multi-stage) and simultaneous mechanisms, on small to large scale distribution networks.

1. Introduction

The growing interest in the decarbonization and stabilization of utility grids have birthed research in transforming the traditional power grid into an efficient smart grid. To this course, different studies have integrated different distributed energy resource (DERs) units into the distribution networks. Renewable energy sources (RES) have been the main focus, to aid a sustainable power grid while reducing carbon footprints. While RES is known for its' setback in continuous power supply, such as variability and intermittency, battery energy storage systems (BESS) are deployed to counter the effects, storing energy for downtime use and regulating the voltage fluctuations (Salama and Chikhani, 1993; Yang et al., 2014). However, these systems are very expensive to install and maintain Awad et al. (2015), and even more, they add to the complexity of the distribution networks, starting from the simulation software modelling to the implementation.

Furthermore, an inappropriate installation of these units can be counter-intuitive to the expected results (Schweppe and Wildes, 1970; Paliwal et al., 2014), hence, previous studies have developed planning framework to allocate multiple unit types in power system networks. These unit types include energy sources and flexible alternating current transmission systems (FACTS) devices, such as photovoltaic distributed generators (PV-DG) units, wind turbines (WT-DG) units, microturbines, BESS, capacitors, voltage regulators, static compensators, and fault detectors.

More recently, electric vehicles (EVs) are the promising technologies to support sustainability and efficiency in modern power system networks, due to their combustion-free energy and capability to feed in real and reactive power into an electrical grid (Zheng et al., 2019). However, their natural charging pattern may cause potential grid collapse (Uddin et al., 2018). Therefore, there is a need to strategically coordinate these charging,

☆ This research was partially supported by the Council for Scientific and Industrial Research, Pretoria, South Africa, through the Smart Networks collaboration initiative and IoT-Factory Programme, South Africa (Funded by the Department of Science and Innovation (DSI), South Africa), and partially by South Africa's National Research Foundation (114626, 112248, and 129311).

* Corresponding authors.
E-mail addresses: kayvins@gmail.com (K.E. Adetunji), ivan.hofsajer@wits.ac.za (I.W. Hofsajer), a.abumahfouz@ieee.org (A.M. Abu-Mahfouz), ling.cheng@wits.ac.za (L. Cheng).

https://doi.org/10.1016/j.egyr.2022.10.379

Table 1
A chronological taxonomy of smart grid planning frameworks involving multiple unit type allocation.

Ref.	Year	Algorithm	MOO	Planning mode	Planning mechanism	DG	BESS	CB	EVCS	VR
(Rodríguez-Gallegos et al., 2018)	2018	GA	Pareto	Loc. & size	Simultaneous	✓	✓			
(Wong et al., 2019)	2019	WOA	✗	Loc. & size	Simultaneous	✓	✓			
(Singh et al., 2020a)	2020	CMSO	✗	Loc. & size	Simultaneous	✓	✓			
(Bozorgavari et al., 2019)	2019	LP solver	✗	Allocation & EMS	Sequential	✓	✓		✓	
(Mukhopadhyay and Das, 2020)	2020	PSO	✗	Loc. & size	Sequential	✓	✓			
(Erdinc et al., 2018)	2020	SOCP solver	✗	Loc. & size	Simultaneous	✓	✓		✓	
(Gampa et al., 2020)	2020	GOA	WSA	Loc. & size	Simultaneous & Sequential	✓		✓	✓	
(Abou El-Ela et al., 2021)	2021	equilibrium	✗	Loc. & size	Simultaneous	✓	✓			
(Adetunji et al., 2021)	2021	WOAGA	Pareto	Loc. & size	Dynamic	✓	✓			
(Barukčić et al., 2021)	2021	MIDACO	Pareto	Allocation & EMS	Sequential	✓	✓			
(Biswal et al., 2021)	2021	QRSMA	✗	Loc. & size	Simultaneous	✓		✓		
(Mouwafi et al., 2021)	2021	CBA	✗	Loc. & size	Sequential	✓		✓		
(Janamala and Reddy, 2021)	2021	Coyote	✗	Loc. & size	Sequential	✓	✓			
(Abdel-Mawgoud et al., 2021)	2021	HGSO	✗	Loc. & size	Simultaneous	✓	✓			
(Shaheen and El-Sehiemy, 2020)	2021	EGWA	WSA	Loc. & size	Simultaneous	✓		✓		✓
(Thokar et al., 2021)	2021	CMSO	WSA	Loc. & size	Dynamic	✓	✓			
(Pirouzi et al., 2022)	2022	MILP solver	✗	Loc. & size	Simultaneous	✓	✓			
(Pereira et al., 2022)	2022	GA	✗	Allocation & Automated	Simultaneous	✓		✓		

either by assigning time slots or recommending charging stations. Hence, there is a need to consider the optimal allocation of electric vehicle charging stations (EVCS) in the smart grid planning models.

1.1. Related works

Table 1 shows the taxonomy of previous related studies on smart grid planning regarding the allocation of multiple DER, PE, or EVCS facilities.

We focus on hybrid metaheuristic optimization algorithms since they have played a major role in improving planning framework solutions,. Most studies tap from their unique capabilities to solve the planning problem cooperatively or each algorithm is used to solve different sub-problems. Fang et al. (2022) discusses the advantage of hybridizing metaheuristic algorithms, especially for complex problems like unrelated parallel machine scheduling tasks.

Jeddi et al. (2019) combined the Firefly Algorithm (FA) and the Harmony Search Algorithm (HSA) to increase distribution network companies' profits by increasing income and reducing the operational costs of a distribution system. The developed optimization scheme uses the FA mechanism for a random search and applies the HSA mechanism to search for the optimal utility values in the harmony memory. However, the optimization scheme is reported to be computationally intensive. In order to mitigate high complexity, Barukčić et al. (2021) developed a co-simulation framework to allocate DG units while managing DG power. In the quest to develop a robust optimal allocation model that finds optimal solutions while reducing computational complexity, the authors applied an artificial neural network to reduce the number of decision variables before finding optimal values, which is done by simultaneously outputting optimal solutions through one vector.

Given the longevity of power system networks, it is crucial to have an extensive smart grid planning model; a model that involves multiple DER units and/or FACTS devices. Previous studies on the smart grid have considered two or more of these elements. Rodríguez-Gallegos et al. (2018) proposed a novel method to allocate multiple, different DER units - PV-DG, BESS, and diesel generators. The procedure is based on a sequential planning mechanism that first considers finding the total BESS power and not considering power losses while defining a fixed PV power through a time horizon into the distribution network. Mouwafi et al. (2021) developed a two-stage approach to solve a multiple DG units and capacitors problem. The adopted approach is similar to the sequential mechanism, using optimal capacitor locations for optimally allocating DG units in a 34- and 118-bus distribution network. The authors applied a chaotic BAT algorithm to single objective and multi-objective functions. However, the mechanism is chosen arbitrarily, with no motivation.

Gampa et al. (2020) used the simultaneous and sequential mechanisms to allocate DG units, capacitors, and EVCS facilities in the distribution network, implementing a weighted sum assignment (WSA)-based MOO framework to optimize objective functions. The DG and capacitors are simultaneously allocated in the first stage, followed by the allocation of EVCS facilities, making it sequential to the first stage. In Singh et al. (2020b), a simultaneous approach was proposed to allocate multiple unit types optimally — PV-DG, shunt capacitors, and on-load tap changers. This approach combines all decision variables into a single one-dimensional vector, making the computation less expensive. However, no investigation was carried out on the strength of the mechanism. Although Biswal et al. (2021) identified the lack of simultaneous planning mechanism in literature, there was no comparative study on the developed mechanism with the sequential mechanism. They however varied the power factor while finding the optimal location and sizes of DG units and capacitors.

Some studies also investigated the effect of different variables on installed DER and FACTS units. For example, Janamala and Reddy (2021) implemented a robust optimal DG and BESS model that considers the varying nature of EV loads while finding optimal DG/BESS locations and sizes. Abou El-Ela et al. (2021) varied the number of PV-DG units and BESS units, and BESS state of charge limits to the optimal allocation suitable for a 33-bus distribution network. In Pereira et al. (2022), a simultaneous planning mechanism was used to allocate DG and capacitor units, considering the effects of applying the sequential Monte Carlo technique to correlate stochastic historical data. The binary GA is used to optimize the annual loss and investment cost reduction.

Wong et al. (2019) investigated the comparison of a two-step and a simultaneous approach to allocate PV-DG and BESS units in the IEEE 33-bus distribution network. However, both approaches are not based on planning mechanism, but rather a method that allocates only BESS units regarding their locations and sizes.

Dynamic planning mechanism is another mechanism that has been scarcely implemented in literature. Although very computationally expensive, it is effective for finding improved solutions since it generates a larger solution space. Pirouzi et al. (2022) considered proposing a dynamic planning model that will allocate DG units and capacitors in future work. Thokar et al. (2021) developed a nested dynamic mechanism that dynamically allocates BESS units given the group installation of solar PV panels in a

planning framework. Using the CMSO, the optimal coordination of the BESS units is achieved, considering the WSA-based optimization of objective functions. In Adetunji et al. (2021) and Adetunji et al. (2022), a dynamic planning mechanism was implemented to allocate multiple DER and FACTS units in smart grid planning framework. However, the optimality of the objective functions was traded off for a high computational time.

As seen in the review, most smart grid planning frameworks involving multiple DER, FACTS, or EV charging station allocation are optimized either using a sequential or a simultaneous planning mechanism. However, to the best of our knowledge, little attention is paid to the effect of the planning mechanism and the application of dynamic planning mechanisms in smart grid planning frameworks. This paper goes beyond the literature by investigating the impact of planning mechanisms in planning frameworks, specifically improving on the proposed dynamic planning mechanism in Adetunji et al. (2021). While our proposed planning mechanism is hypothesized to reduce computational complications from previous studies, the challenging conditions are the potential residual complexities from the multiple iterations of unit allocations. To handle these complexities, we proposed a novel adaptive dynamic planning mechanism in a multiple unit type allocation planning frameworks. The contributions are summarized as follows

1.2. Contributions

In this paper, we develop a planning framework by optimally allocating multiple unit types to a distribution network. The framework consists of various objectives, hence adopting a MOO technique to find compromise solutions that represent all adopted objectives in the view of a decision-maker. The paper contributions are

- *Adaptive Dynamic Planning Mechanism*: We design a novel adaptive-dynamic planning mechanism as an underlying blueprint for use by an optimization scheme to solve the planning problem. Unlike other conventional mechanisms used in Gampa et al. (2020), Biswal et al. (2021) and Mouwafi et al. (2021), the dynamic mechanism uses a recombination technique that considers the feedback of other unit types to expand the solution space.
- *Hybrid Evolutionary Optimization Scheme*: We develop a hybrid cooperative spiral-based genetic algorithm and differential evolution (CoSGADE) optimization scheme based on the newly designed planning mechanism. The scheme decomposes the problem, splitting the whole problem into sub-problem and using each algorithm at different stages of the optimization process. The CoSGADE is implemented in two forms, hoping to solve the complex model in a considerably reasonable computational time.
- *EVCS Allocation*: We introduce a reinforcement learning-based allocation scheme, using the results from the EV charging strategy to suggest optimal EVCS locations in distribution networks. A reinforcement learning technique is introduced to find the optimal EV charging strategy for different bus locations.

1.3. Paper outline

The rest of the paper follows the structure - Section 2 discusses the different planning mechanisms. Section 3 discusses the integration model and the problem description, entailing the objective functions, constraints, and the MOO technique. Next, Section 4 discusses the solution methodology, entailing the proposed dynamic planning mechanism and the new optimization technique, the CoSGADE. Finally, Section 5 discusses the numerical results, while Section 6 presents the conclusions from the study.

2. Planning mechanisms

First, to understand the concept of planning mechanism, we need to define the low-level problem, starting with unit type.

Definition 1. In this paper, unit type is defined as the category of DER or FACTSunits according to their functionality to the grid. For example, a DG unit is a unit type that supplies power to the grid irrespective of the generation source, e.g., Wind, Solar, Diesel, etc.; hence, any form of DG unit is categorized as a unit type. A BESS unit is another unit type since its operation is coordinated to optimally charge and discharge to and from the grid, primarily dependent on renewable-based DG units. Other unit types that can be optimally allocated are capacitors, voltage regulators, fault limiters, and EVCS facilities.

Definition 2. In this paper, planning mechanism is defined as the underlying design in a planning framework to allocate more than one unit type in a power system network. The optimization scheme uses the design to find the optimal planning scheme. Planning mechanisms are more significant when two or more unit type allocation is considered for a smart grid planning framework.

There are three conventional planning mechanisms for allocating multiple unit types: preallocated, sequential, and simultaneous. The preallocated form of mechanism involves allocating one unit type into a distribution network earmarked with one or more different unit type(s). An example is finding optimal BESS locations and sizes in the presence of PV-DG and capacitor units. The step for allocating PV-DG and capacitors will be skipped, assuming they are optimally allocated, only to focus on allocating the BESS units. This method is very straightforward and less complex, but the assumption that earmarked units are optimally allocated can be costly to derive optimal solutions.

The sequential form of mechanism is allocating multiple unit types in successive order. The first unit, e.g. a capacitor, is singularly allocated, followed by another distinct unit type, e.g., the BESS unit. This mechanism ensures that, within the optimization framework, unit type allocation is dependent on the effect of previously allocated unit type on the distribution network. The simultaneous mechanism allocates all unit types together in one iteration. The location and size of all unit types are manipulated at once, considering the utility value as the fitness value to determine the optimal allocation variable per iteration. The drawback is a limited number of iterations to find the best permutation among unit types. Increasing the number of iterations will be counter-intuitive to the simplicity of the mechanism.

The other form of planning mechanism is the dynamic mechanism, where the permutation of unit location is considered. This mechanism has only been reported in Thokar et al. (2021) and Adetunji et al. (2021). Fig. 1 shows the visual illustration of the proposed mechanisms.

As seen in Fig. 1, the preallocated mechanism involves the most minimal form of manipulating allocation variables, making it the most straightforward approach. The simultaneous form is next in simplicity, as it manipulates all variables in one iteration. Finally, the proposed dynamic mechanism is adapted from the sequential form but adds a cyclic process to involve sub iterations in the main iteration cycle.

3. Problem formulation

In this section, a multi-objective optimal allocation problem consists of multiple different DER technologies and FACTS devices aiming to optimize adopted objective functions in a smart grid planning framework. In addition, some terminologies are predefined in the planning framework. The adopted objectives and constraints are discussed in the following subsections.

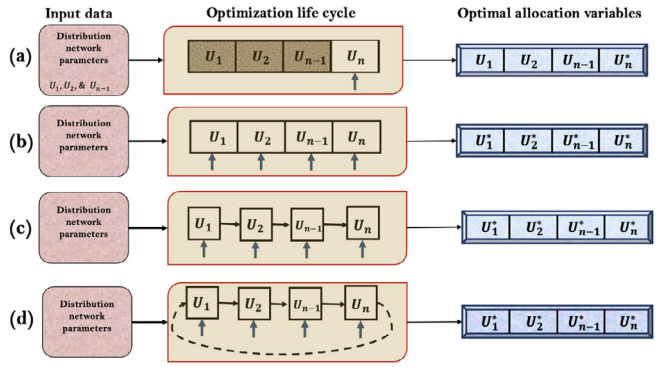

Fig. 1. Mechanisms for smart grid planning models (a) preallocated mechanism. (b) simultaneous mechanism. (c) sequential mechanism. (d) dynamic mechanism.

3.1. Objective functions

The objective of the planning model is to improve grid performance which has been formalized by adopting three objective functions — power loss minimization, voltage stability improvement, and voltage deviation reduction. The objective functions are defined as follows.

3.1.1. Power loss minimization

One of the primary objectives of a utility grid is to deliver maximum power from the source to all nodes in a power system network. To achieve maximum power delivery, power loss within the network has to be minimized as best as possible. we, therefore, consider the power loss minimization as one of the objectives, defined as

$$P_t^{\mathrm{LOSS}} = \sum_{i=1}^{N}\sum_{j=1}^{N} \alpha_{ij}\left(P_i^t P_j^t + Q_i^t Q_j^t\right) + \beta_{ij}\left(Q_i^t P_j^t - P_i^t Q_j^t\right) \tag{1}$$

where

$$\alpha_{ij} = \frac{r_{ij}}{V_i V_j} cos\left(\delta_i - \delta_j\right) \tag{2}$$

and

$$\beta_{ij} = \frac{r_{ij}}{V_i V_j} sin\left(\delta_i - \delta_j\right). \tag{3}$$

Here, i and j are the sending and the receiving bus indices, respectively, while $Z_{ij} = r_{ij} + jx_{ij}$ represents the branch impedance from bus i to bus j, P and Q are the real and reactive power at each bus.

3.1.2. Voltage deviation reduction

Delivery of power also comes with the assurance of quality. Power quality is affected by the deviation of voltage from the tolerance range, which can be aggravated by newly installed units. Hence, the second objective is to reduce the voltage deviation at each bus and described as

$$VD = \sum_{i=2}^{N} |V_i^t - V_{ref}|, \tag{4}$$

where the reference voltage, V_{ref} is set at one and V_i represents the voltage at each bus after the addition of DG or BESS units.

3.1.3. Voltage stability improvement

Another crucial indicator for evaluating grid performance is the voltage stability of the network. High penetration of power from DER units to certain buses can destabilize the whole network; hence there is a need to consider this index while finding optimal planning variables. We expressed the voltage stability improvement as

$$\begin{aligned} vsi_{i+1,t+1} &= \left(|V_{i,t}|^2 - 2P_{i,t}R_{i,t} - 2Q_{i,t}X_{i,t}\right)^2 \\ &\quad -4\cdot\left(P_{i,t}^2 + Q_{i,t}^2\right)\cdot\left(R_{i,t}^2 + {X_{i,t}}^2\right), \end{aligned} \tag{5}$$

$$VSI_{i,t} = \frac{1}{\min(vsi_{i+1,t+1})}, \tag{6}$$

$$VSI = \frac{1}{24}\sum_{i=2}^{N}\sum_{t=1}^{24} VSI_{i,t}. \tag{7}$$

3.2. Constraints

A power system network has many constraints that guide its smooth operation. Therefore, there is a need to formulate necessary constraints to improve the practicality of the optimal unit allocation model.

$$P_i^t = \sum_{j=1,j\neq i}^{N} Y_{ij}V_i^t V_j^t \cos(\theta_{ij} + \delta_j - \delta_i) \tag{8}$$

and

$$Q_i^t = \sum_{j=1,j\neq i}^{N} Y_{ij}V_i^t V_j^t \sin(\theta_{ij} + \delta_j - \delta_i). \tag{9}$$

Although there was no injection of reactive power from PV-DG unis, it is necessary to monitor boundaries during the injection of real power.

The operating voltage at every bus must satisfy the range at all buses. The admittance on a branch is represented as Y_{ij}. The bus voltage limit is formulated as

$$V_i^{\min} \le V_i \le V_i^{\max} \quad i = 1, 2, \ldots, N, \tag{10}$$

where V_i is the current voltage at bus i. The tolerance level of voltage is ±5%, therefore V_i^{min} and V_i^{max} are 0.95 and 1.05 respectively.

The power flow balance is also considered. The total real power generation (from all DG and BESS units) must equal the total real load, total real power loss, and the BESS charging and discharging power (Kansal et al., 2013). Therefore, a balance of the power flow is calculated as

$$P_{i,t}^{\mathrm{DG}} + P_{j,t}^{\mathrm{Dis}} = P_{i,t}^{\mathrm{LOSS}} + P_{i,t}^{\mathrm{LOAD}} + P_{j,t}^{\mathrm{Ch}}, \tag{11}$$

where the $P_{j,t}^{\mathrm{Dis}}$ and $P_{j,t}^{\mathrm{Ch}}$ represent the BESS discharging and charging power to and from the grid from bus j at time t.

3.2.1. BESS constraints

This paper selected the Lead–acid battery technology due to its economic viability and reliability since they have a considerably high tolerance for overcharging. For a practical scenario, the BESS model is subject to *state of charge SoC* limit, which prevents excessive charging or discharging from the battery and defined as (Das et al., 2018)

$$SoC^{min} < \frac{E_t^B}{E_t^{BA}} < SoC^{max}, \tag{12}$$

where the SoC^{min} and SoC^{max} are 0.2 and 0.9 respectively. The charging and discharging power are specified as (Das et al., 2019; Kaur et al., 2019)

$$E_{t+1}^B = \begin{cases} E_t^B - P_t^B \Delta t \eta_{Bc} & P_t^B \le 0 \\ E_t^B - \frac{P_t^B \Delta t}{\eta_{Bd}} & P_t^B > 0 \end{cases}, \tag{13}$$

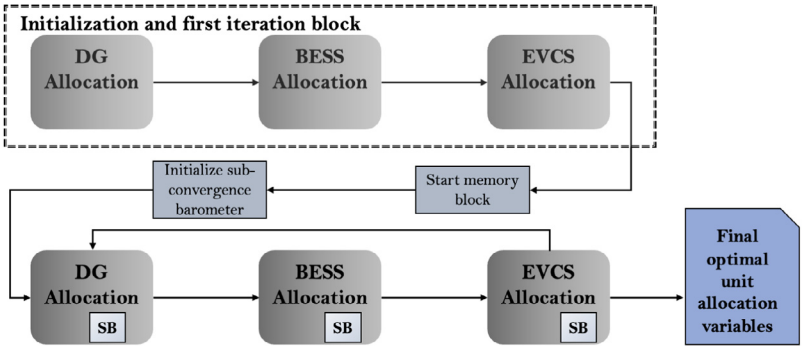

Fig. 2. Block diagram for the adaptive dynamic planning mechanism.

where E_t^B is the energy of the BESS unit at time t, P_t^B is the charging power of the BESS unit at time t, Δt is the time interval, η_{Bd} and η_{Bc} are the discharging and charging efficiency of the BESS unit respectively, the battery power is limited by

$$E^{\min} \leqslant E_{i,t}^B \leqslant E^{\max}, \tag{14}$$

where $E_{i,t}$ is the energy of the ith BESS unit at time t.

Given that most EVs use a lithium-ion battery, this study modelled a lithium-ion battery, which injects current to a bus at a given time. The current is expressed as

$$I_i = \frac{(P_i^t + Q_i^t)}{V_i^t}, \tag{15}$$

where P_i and Q_i are the real and reactive power at bus i at time, t. V_i^t is the bus voltage at bus k at time, t. The reactive power Q_i^t will always be zero at every time, t, since only real power will only be considered.

3.2.2. Capacitor constraints

The capacitor banks are also bounded by maximum sizes, given as

$$CAP^{\min} \leqslant CAP_i \leqslant CAP^{\max} \tag{16}$$

3.2.3. EVCS constraints

The EVCS is modelled as a load, according to the EVs roaming to charge in a network. Therefore, EVCS facilities must not exceed the total EV load and distributed evenly across all EVCS facilities, hence having the same capacity. The constraint is represented in (17)

$$\sum P_{i,t}^{\text{EV}} \leqslant \sum P_k^{\text{EVCS}} | N(\mu, \sigma), \tag{17}$$

where $\sum P_k^{\text{EVCS}}$ is the charging of the kth EVCS that follows a normal distribution of a mean and standard deviation across all EVCS.

3.3. Multiobjective approach

The adopted objective functions are processed simultaneously processed using the weight sum aggregate method. The weights indicates the level of preference and are equally distributed to all objective functions. Therefore, $w_1 = w_2 = w_3 = 0.33$. The final value represents the utility value of the model, which is used to determine the fitness value in the optimization process. The utility value is expressed as

$$U = w_1 P^{\text{LOSS}} + w_2 VD + w_3 VSI. \tag{18}$$

To standardize the problem as minimization problem, we used the inverse of VSI, shown in (6).

4. Solution methodology

4.1. Proposed adaptive dynamic planning mechanism

This section seeks to address the gap observed in the literature, as in Sections 1.1 and 2, by proposing an adaptive dynamic mechanism to increase potential solutions for the optimal multiple DER allocation problem. Already established that the dynamic planning mechanism performs better than other planning mechanisms, but with intense computational time, we introduce a sub-convergence barometer that monitors the sequence of values to determine the convergence in each stage of the optimization process. The barometer works with a memory block, which stores the last best fitness values of the previous ten iterations. The algorithm sub-converges and moves to the next stage if the fitness value remains the same with ± 0.005 tolerance. The process of the convergence barometer and the memory block can be seen in Fig. 2.

With SB representing the sub-convergence barometer in Fig. 2, it is seen that the barometer and the memory block starts at the second iteration of the whole allocation process. The barometer fastens the optimization process by helping to quickly move out of an allocation when there is no improvement in the fitness value. The effect of this function is illustrated in the results section, Section 5.6.

4.2. Heuristic proof

Using the Big $\mathcal{O}$ notation complexity analysis, we show the difference in complexity for different planning mechanisms (independent of the optimization algorithm) on the mixed-integer linear problem-based smart grid planning problem. Given that we have N_i is the number of variables for a variable type i, T, the number of processes (or iterations), and number of constraints and uncertainties are constant across all planning mechanism modes, the notation for sequential will be $\mathcal{O}(T\frac{N_i}{2} + TN_i)$ which sums to $\mathcal{O}(2T\frac{3}{2}N_i)$. The simultaneous planning mechanism is $\mathcal{O}(TN_i)$, while the dynamic mechanism is $\mathcal{O}(T^2N_i)$. The adaptive form yields $\mathcal{O}((T-p)^2N_i)$, where p, an absolute value always lesser than T, is the remainder of the number of iterations when there is a sub-convergence.

4.3. Hybrid optimization strategy

CoSGADE is a hybrid evolutionary algorithm developed to handle large scale optimization problems, such as the optimal planning of smart grid networks. The high-level approach is to divide the planning framework into sub-iterations of different unit allocations, shown in Fig. 3

As seen in Fig. 3, the first vector contains DG locations and sizes while the second and third vectors accommodates the BESS

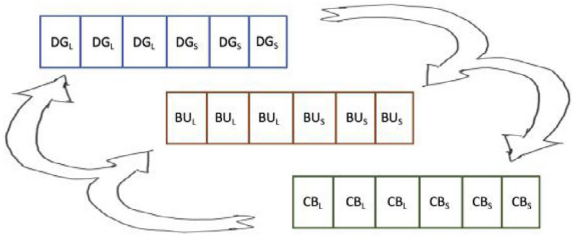

Fig. 3. High-level process of the planning optimization scheme.

units (BU) and capacitor banks (CB) respectively. Each of these vectors are solved at a sub-iteration level. The lower level of the optimization scheme uses two evolutionary algorithms, namely the DE and GA, to solve the planning problem cooperatively. The problem is split into two sub-problems: (i) discrete variable, which handles the location of units, and (ii) continuous variables, which involve the sizing of the units. Given its effective capability to manipulate discrete variables, the GA is dedicated to solving optimal unit locations. The DE, on the other hand, uses a similar approach but with some extra parameters that make it efficient for manipulating continuous variables. The DE also models the solution variables as chromosomes, with each gene representing a unit type size. Finally, the DE uses a scaling factor to ensure positive integers during the mutation process in addition to the GA's operator.

The DE's mutation operator also differs from the traditional GA because it uses the difference of parent vector (or chromosome). While the DE is effective, simple, and less complex to implement, it often suffers from stagnation due to the complexity of manipulating continuous large-scale optimization problems (Islam et al., 2012; Das and Suganthan, 2011). Stagnation is a common drawback in stochastic search algorithms, where results are no longer improved during the iteration process, even when there are better solutions in the solution space. A spiral mechanism is adopted to overcome this drawback, adapted from the WOA (Mirjalili and Lewis, 2016) due to its effective finding of optimal solutions in a relatively quick manner. The CoSGADE's search operator is then maintained by implementing a probabilistic roulette wheel that controls the switch between the DE's search and the spiral search for every new generation. Eq. (19) shows the illustration of the CoSGADE's search mechanism.

$$X_{i,G+1} = \begin{cases} X^{\mathrm{DE}}, & p < 0.5 \\ X^{\mathrm{rand}} - D \cdot e^{bl} \cdot \cos(2\pi l) & p \geqslant 0.5 \end{cases}, \tag{19}$$

where $[X_{i,G+1} | \forall x^d_{i,G} \in x^D_{i,G}]$ is ith vector solution for the next generation, $G+1$ and d is the variable (gene) in the vector (chromosome). The randomly spiralled phase occurs when the roulette wheel produces a $\geqslant 0.5$ probability value. This phase diversifies the search away from local optima, using the X_{rand}. The D parameter represents the distance between the current vector solution and the best vector solution, expressed as $D = |C \cdot X^*_G - X_G|$, where $C = 2 \cdot r$ is a random parameter that is updated at every generation.

The DE's manipulation process starts with the mutation process, creating a donor vector, represented as

$$V_{i,G} = X^*_G + F(X_{r^1_{i,G}} - X_{r^2_{i,G}}), \tag{20}$$

which corresponds to each target vector, $X_{i,G}$. The r^i_1 and r^i_2 are mutually exclusive random integers peculiar to every iteration; the scaling factor, F, is a control parameter to ensure positive integers while calculating the difference donor vector. The crossover operator is performed on $V_{i,G}$, manipulating its solution variables to form a trial vector, $U_{i,G} | \forall u^d_{i,G} \in u^D_{i,G}$. The vector is determined using

$$U^d_{i,G} = \begin{cases} v^d_{i,G}, & \text{if } z \leqslant Cr \\ x^d_{i,G}, & \text{otherwise} \end{cases} \tag{21}$$

where z is a uniformly distributed random parameter between 0 and 1, called anew for manipulation of each d_{th} variable of the i_{th} vector of population in generation G. The z parameter also ensures that $U_{i,G}$ gets at least one solution variable from $X_{i,G}$. Finally, the selection process determines the surviving vector to the next generation, $G+1$, shown as

$$X_{i,G+1} = \begin{cases} U_{i,G}, & \text{if } f\left(U_{i,G}\right) \leqslant f(X_{i,G}) \\ X_{i,G}, & \text{if } f\left(U_{i,G}\right) > f(X_{i,G}) \end{cases} \tag{22}$$

where $f(\cdot)$ is the utility function value for a known vector of allocation variables.

Having explained the CoSGADE mechanism and the dynamic modelling, the optimization scheme will obviously suffer a high complexity. Firstly, the recombination technique uses more iterations to converge. Secondly, the operation or effect of the units to be allocated has to be carried at T number of iterations. Hence, we propose two implementations for applying the CoSGADE optimizer to mitigate this setback.

CoSGADE-I. Here, the process involves the optimization of each unit type in a sub-iteration. This process indeed requires a high computational time which increases drastically according to the number of unit types to be allocated. To overcome the limitation, the CoSGADE is incorporated with a convergence barometer and a memory block. Fig. 4 illustrates the process. As seen in Fig. 4, the memory block is initialized after the first round of iterations, beginning the storage of utility values. Then, the convergence barometer is implemented to utilize the memory block, computing the difference in utility values across every ten iterations. A nominal value terminates the current sub-iteration, i.e., suspending the optimizer to use optimal unit type allocation solutions in the memory block. This process significantly reduces computational time. The capacitor allocation module involves an optimization process similar to PV-DG and BESS allocation process. It is to note that other unit types, e.g., EVCS, can easily be replaced or added to the optimization scheme.

CoSGADE-II. To achieve the control mechanism that checks different unit type allocation against each other, it is proposed to have one vector representing all the allocation variables, but arranging the vector such that the location and size of all unit types are categorized. The mechanism uses each algorithm for a sub-iteration, containing distinct variable types. Here, the location is first optimized by the GA then the final solution of the sub-iteration is pushed to DE for the size to be optimized. The process is repeated until convergence is reached. Fig. 5 illustrates the procedure.

It is observed in Fig. 5 that there are fewer steps, which translates to a faster computational time. Compared to CoSGADE-I, the unit locations are checked against their sizes at every iteration. The solution vectors in a population are represented as follows.

$$\overrightarrow{X}_G = \begin{pmatrix} x^{\mathrm{L}}_{1,1} & \cdots & x^{\mathrm{L}}_{D,1} & x^{\mathrm{S}}_{1,1} & \cdots & x^{\mathrm{S}}_{D,1} \\ x^{\mathrm{L}}_{1,2} & \cdots & x^{\mathrm{L}}_{D,2} & x^{\mathrm{S}}_{1,2} & \cdots & x^{\mathrm{S}}_{D,2} \\ \vdots & \ddots & \vdots & \vdots & \ddots & \vdots \\ x^{\mathrm{L}}_{1,M} & \cdots & x^{\mathrm{L}}_{D,M} & x^{\mathrm{S}}_{1,M} & \cdots & x^{\mathrm{S}}_{D,M} \end{pmatrix}, \tag{23}$$

where $x^{\mathrm{L}}_{1,1}$ is the first unit type location of the first chromosome, given a total number of D unit types sizes in M number of population. $x^{\mathrm{S}}_{1,1}$ represents the sizes in the same context.

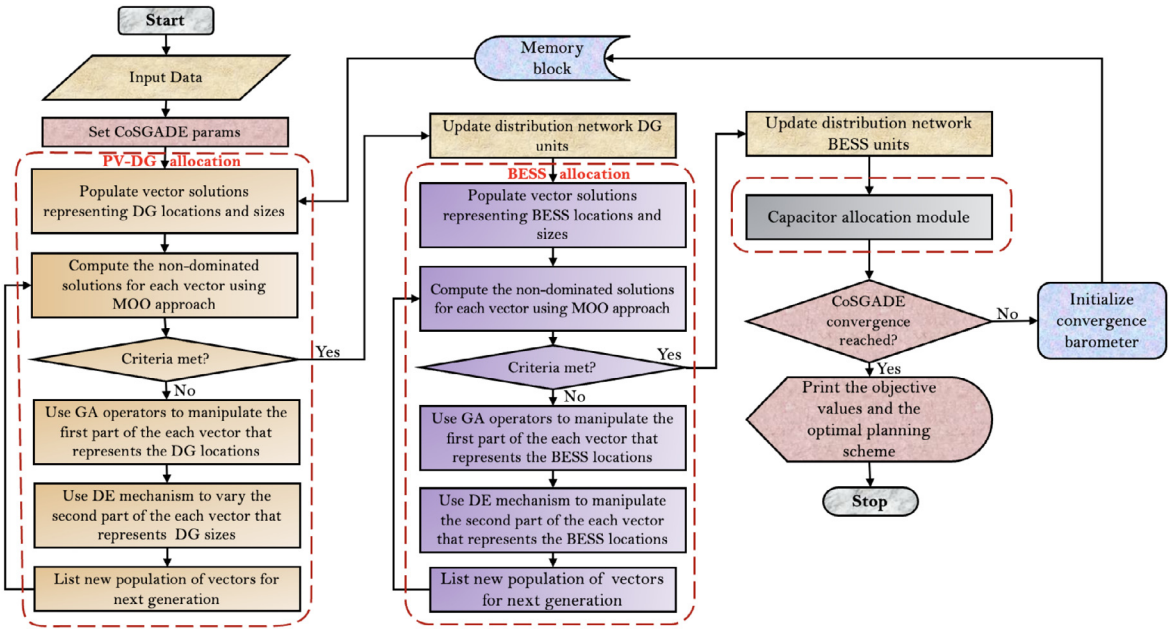

Fig. 4. Flowchart of the first implementation of the CoSGADE optimization scheme.

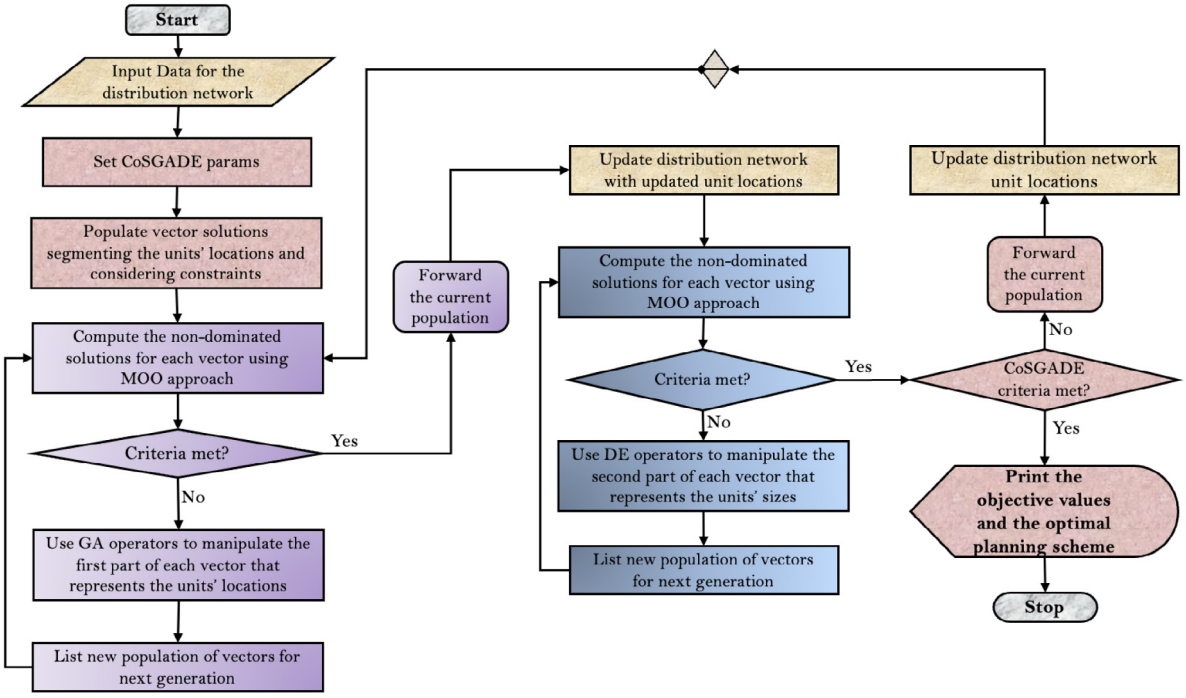

Fig. 5. Flowchart of the second implementation of the CoSGADE optimization scheme.

4.4. EVCS allocation model using reinforcement learning

This section discusses the allocation of the EVCS facilities into distribution networks. The problem is formed based on a Markov Decision Process, in which the optimum performance of the grid is determined by the EVCS locations that produce the best control strategy. Algorithm 1 shows the procedure of the EVCS allocation scheme.

The MDP structure is depicted as $\mathcal{M} = \langle \mathcal{S}_t, \mathcal{A}_t, \mathcal{R}_t, T, \gamma \rangle$, where state $\mathcal{S}_t = \langle \mathcal{I}_t, d_s \rangle$ given $\mathcal{I}_t$ is the set of EV chargers drawing power from the distribution network, d_s is the power demand in the network. The action, $\mathcal{A}_t = \langle a_{\text{EVCS}} \rangle$, where a_{EVCS} is the set of EVCS allocated to EV drivers. The reward, $\mathcal{R}_t$ offered to the agent that takes action $\mathcal{A}$ in state $\mathcal{S}$ is measured using (24), to be used for the next state, $\mathcal{S}+1$. The probability of transitioning from state $\mathcal{S}$ to the next state, $\mathcal{S}+1$ is expressed as

$$T = f(\mathcal{S}, \mathcal{A}, L_t). \tag{24}$$

Therefore, the outcome of carrying out all actions in different states yielding rewards will follow policies π, represented as

$$Q^{\pi}(\mathcal{S}_t, \mathcal{A}_t) = \mathcal{E}[\mathcal{R}_t(\mathcal{S}_t, \mathcal{A}_t) + \gamma Q^{\pi} p(\mathcal{S}_{t+1}, \mathcal{A}_{t+1})], \tag{25}$$

where $\gamma = \{0, 1\}$ is the discount factor that offers rewards for actions over an expectation $\mathcal{E}$ given a time horizon, T. Given

Algorithm 1 EVCS Allocation Scheme

Initialize maximum number of generations G
Initialize a population P of chromosomes, $V = \{v_1, v_2, \ldots, v_n\}$, as the EVCS locations
Set voltage stability as the fitness value of each chromosomes
  while $g < \mathbb{G}_{max}$ **do**
    for all $V \in P$ **do**
      procedure EV_Charge_control(V)
      Sort best chromosome, V^* in the current generation $g++$
    end for
  end while
  Print chromosome with best fitness from the control strategy
  $V \leftarrow V^*$
  return V

Eq. (25), an optimal policy which maximizes the grid performance the most is expressed as

$$Q^*(\mathcal{S}, \mathcal{A}) = \max_{\pi} Q^{\pi}(\mathcal{S}_t, \mathcal{A}_t) \tag{26}$$

This optimal policy is learned using a recursive algorithm to update the state–action pairs, mapped as

$$Q^*(\mathcal{S}_t, \mathcal{A}_t) = (1-\alpha)Q(\mathcal{S}_t, \mathcal{A}_t) + \alpha[Q^{\pi}(\mathcal{S}_t, \mathcal{A}_t)], \tag{27}$$

where α is the learning rate of the algorithm, chosen between 0 and 1. Algorithm 2 shows the SARSA learning procedure for the control problem.

Algorithm 2 SARSA-Learning Algorithm

Initialize number of episodes, $\mathbb{E}$
Initialize the EV charging demand for set of EVs as state $\mathcal{S}$
Initialize EVCS location selection as action $\mathcal{A}$
Set power loss (1) as reward $\mathcal{R}$
  while $e < \mathbb{E}$ **do**
    Collect distribution network and EVCS features to realize state, $\mathcal{S}$
    Select action $\mathcal{A}$ from $\mathcal{S}$
    Receive reward $\mathcal{R}$, receive new data, and generate next state $\mathcal{S}+1$
    Update $Q(\mathcal{S}, \mathcal{A})$ using (25)
    Find the optimal policy using (26) and learn this policy using (27)
    $\mathcal{S} \leftarrow \mathcal{S}+1$
    Terminate at desired state $e++$
  end while
  Output the best policy $\boldsymbol{\pi}$

5. Numerical analysis

In order to demonstrate the efficiency and practicality of the proposed planning framework, we evaluate the proposed adaptive-dynamic mechanism and the CoSGADE optimization on a 15-bus, IEEE 69-bus and 118-bus test distribution network. The load consumption is processed as a probability density function, to handle uncertainties from consumers' daily and seasonal behaviour. The same technique is applied to PV power output through the modelling of the solar irradiance and temperature data. The simulation was carried out using MATLAB® 2022 on an Intel® Core™ i7-10510U 16 GB RAM CPU @ 1.80 GHz and 2.30 GHz.

Table 2
Different cases for numerical analysis.

Case	PV-DG & BESS	CB	EVCS
Case 1	✓	✗	✗
Case 2	✓	✓	✗
Case 3	✓	✓	✓

5.1. Evaluation of the planning optimization framework

For a robust explanation of the proposed mechanism's efficiency on solving the planning problem, we draft the analysis into 3 cases. Table 2 shows the cases.

It is to note that the EVCS is a function of the number of EVs to be charged, which must not exceed the combined total capacity of EVCS facility in the distribution network. Hence, the size of EVCS is the product of EV chargers (11.2 kW) and the total number of EVs. Each case is analysed for three study systems — 15-bus, IEEE 69- and 118-bus test distribution network. All cases are analysed using a single objective framework, with power loss minimization as the objective function. We adopted some conventional optimization algorithms to test the proposed CoSGADE on the study systems using the proposed underlying proposed dynamic mechanism.

5.2. Study system I

This study involves the evaluation of the planning model on the IEEE 15-bus distribution network; a 11 kV, 100 KVA base KVA, with a real and reactive power of 1226.400 kW and 1251.178 kVAr, respectively. The three cases are implemented for this system, with the results shown in Table 3.

From Table 3, it is observed that Case 3 has the most power loss and minimum network voltage, given that a multitude of EVs is added to the distribution network model. However, the CoSGADE optimization scheme shows a better performance than the adopted schemes, indicating an improved power loss minimization of 76.7%, 83.8%, and 76.7%, respectively for cases 1 to 3. The voltage profile is also analysed, shown in Fig. 6. It is seen that the CoSGADE produces the best voltage profile for the network.

5.3. Study system II

This study involves the evaluation of the planning model on the 69-bus distribution network; a 12.66 kV network, with a 3.715MW/2.300MVaR as the real and reactive power respectively. To grasp the strength of the proposed mechanism performance, the simulation results are compared to the conventional mechanism.

Table 4 depicts a similar scenario to Table 3, with Case 3 having the most power loss and minimum network voltage. The CoSGADE optimization scheme also shows a better performance than the adopted schemes, indicating an improved power loss minimization of 78.3%, 86%, and 80.1%, respectively for cases 1 to 3. The voltage profile is also analysed, shown in Fig. 7. It is seen that the CoSGADE produces the best voltage profile for the network.

5.4. Study system III

This study involves the evaluation of the planning model on the IEEE 118-bus distribution network; a 11 kV network, with a 22.710MW/17.041MVaR as the real and reactive power respectively. To grasp the strength of the proposed mechanism performance, the simulation results are compared to the conventional mechanism.

Table 3
Unit allocation variables for the IEEE 15-bus distribution network.

Case	Optimizer	DG Allocation *Location(size(KW))*	BESS Allocation *Location(size(KW))*	CB Allocation *Location(size(KW))*	EVCS Allocation	% PL	VS	VD
I	GA	10(119.56), 4(131.04)	8(92)	–	–	56.1	0.0531	0.9518
	PSO	10(112.11), 11(110.18)	8(84)	–	–	63.2	0.0514	0.9523
	PSOGA	11(129.45), 10(92.21)	8(77)	–	–	71.1	0.0337	0.9775
	WOAGA	15(158.14), 11(114.28)	10(142)	–	–	72.1	0.0204	0.9801
	CoSGADE	11(131.02), 15(128.33)	8(59)	–	–	76.7	0.0161	0.9829
II	GA	10(123.56), 4(138.42)	8(91)	4(120), 8(184)	–	68.9	0.0063	0.9626
	PSO	10(112.09), 11(108.41)	8(79)	4(136), 9(106)	–	73.9	0.0050	0.9694
	PSOGA	11(114.22), 10(94.82)	8(79)	6(186), 12(113)	–	79.8	0.0037	0.9837
	WOAGA	15(147.08), 11(112.75)	10(142)	6(177), 12(201)	–	80.7	0.0028	0.9853
	CoSGADE	11(130.76), 15(141.38)	8(55)	3(165), 10(189)	–	83.8	0.0016	0.9881
III	GA	10(269.23), 4(254.42)	8(105)	4(120), 12(197)	3, 7, 12	39.3	0.0645	0.9312
	PSO	10(262.92), 11(275.11)	8(99)	4(166), 9(113)	3, 7, 13	49.7	0.0621	0.9341
	PSOGA	11(230.35), 10(184.57)	8(106)	6(242), 12(201)	3, 7, 12	64.7	0.0456	0.9662
	WOAGA	15(275.62), 11(217.88)	10(137)	6(297), 12(261)	3, 7, 12	67.2	0.0392	0.9665
	CoSGADE	11(272.92), 15(241.38)	8(95)	4(188), 12(222)	3, 6, 12	76.7	0.0311	0.9825

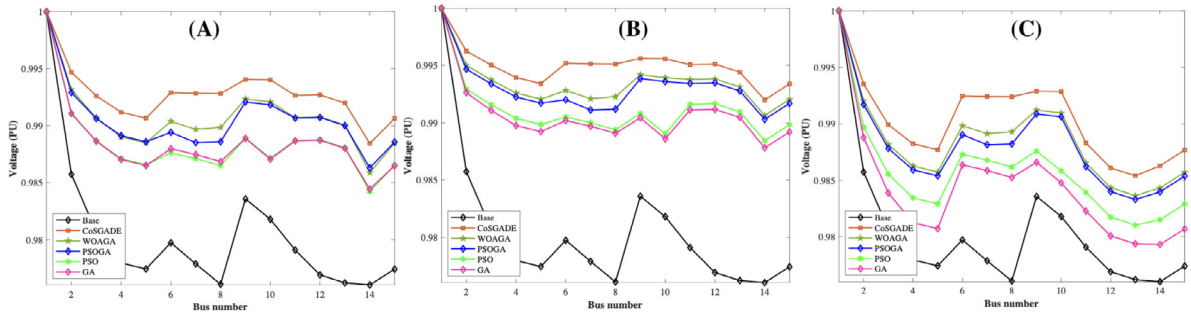

Fig. 6. Study system I voltage profile for all cases (A) PV-DG and BESS allocated to the network. (B) PV-DG, BESS, and Capacitors allocated to the network. (C) PV-DG, BESS, Capacitors, and EVCS allocated to the network.

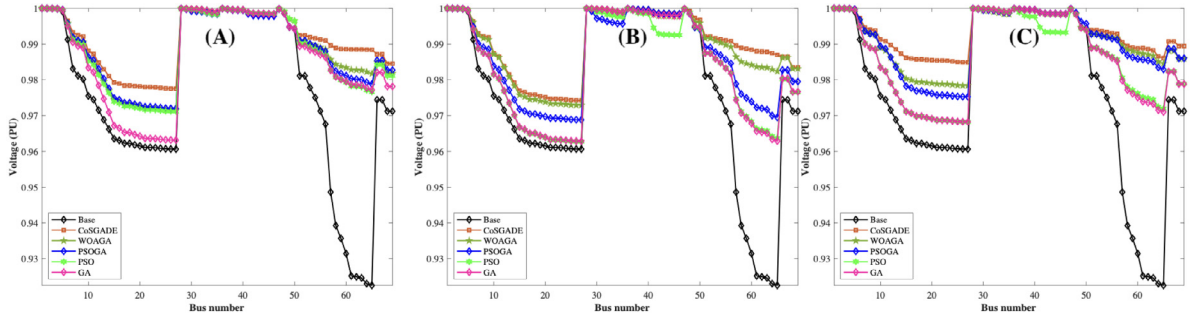

Fig. 7. Study system II voltage profile for all cases (A) PV-DG and BESS allocated to the network. (B) PV-DG, BESS, and Capacitors allocated to the network. (C) PV-DG, BESS, Capacitors, and EVCS allocated to the network.

The CoSGADE optimization scheme in Table 5 shows a familiar improvement as in Tables 3 and 4. An observation is the large scale problem difficulty for the optimization schemes, especially with Case 3, the CoSGADE still outperforms other optimizers in reducing power loss., showing 41.4%, 52.7%, and 32.6% minimization for Cases 1 to 3 respectively. The voltage profile is also analysed, shown in Fig. 8. It is seen that the CoSGADE produces the best voltage profile for the network.

5.5. Performance Analysis of the CoSGADE optimization scheme

This section discusses the performance of the proposed optimization scheme, done by comparing the efficiency of the scheme to other traditional optimization methods. The first check is to evaluate the power loss for each case in the 69-bus and 118-bus systems, shown in Figs. 9 and 10 respectively.

Table 4
Unit allocation variables for the 69-bus distribution network.

Case	Optimizer	DG Allocation *Location(size(KW))*	BESS Allocation *Location(size(KW))*	CB Allocation *Location(size(KW))*	EVCS Allocation	% PL	VD	VS
II	GA	12(524.11), 25(509.02), 49(498.12), 62(659.29)	15(382), 63(355)	22(452), 41(376), 60(403)	–	53.7	0.0582	0.9337
	PSO	14(535.56), 25(518.33), 45(513.18), 63(661.77)	21(376), 63(352)	22(451), 40(334), 60(412)	–	54.3	0.0564	0.9351
	PSOGA	10(555.18), 25(500.83), 49(477.22), 66(650.96)	15(382), 66(377)	20(448), 44(386), 64(411)	–	68.9	0.0329	0.9667
	WOAGA	11(592.62), 27(573.92), 52(523.68), 66(689.68)	61(453), 66(468)	22(475), 43(408), 67(442)	–	72.5	0.0167	0.9703
	CoSGADE	12(511.24), 21(521.83), 62(518.89), 61(647.47)	21(385), 68(461)	22(464), 48(374), 64(367)	–	89.4	0.0084	0.9826
III	GA	02(889.15), 29(814.03), 21(877.42), 61(999.48)	15(552), 65(470)	22(591), 36(415), 65(493)	10, 32, 50, 64	41.1	0.0526	0.9229
	PSO	23(902.22), 21(827.63), 60(865.11), 61(998.03)	18(567), 66(478)	22(587), 38(433), 64(497)	08, 21, 55, 64	41	0.0492	0.9254
	PSOGA	49(882.54), 21(793.69), 61(863.52), 60(991.48)	31(492), 62(467)	20(495), 39(483), 65(567)	10, 32, 52, 64	66.1	0.0341	0.9383
	WOAGA	12(899.75), 50(801.15), 21(831.22), 61(986.59)	62(457), 65(492)	21(492), 37(498), 68(594)	10, 28, 52, 64	65.6	0.0298	0.9478
	CoSGADE	12(781.75), 29(834.03), 61(849.52), 21(993.72)	62(452), 61(483)	22(499), 46(558), 69(592)	14, 28, 52, 64	79.3	0.0184	0.9625

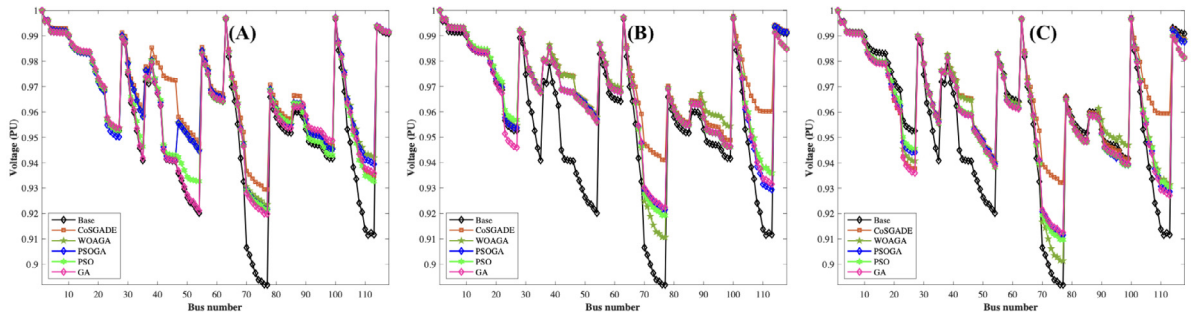

Fig. 8. Study system III voltage profile for all cases (A) PV-DG and BESS allocated to the network. (B) PV-DG, BESS, and capacitors allocated to the network. (C) PV-DG, BESS, capacitors, and EVCS allocated to the network.

In Figs. 9 and 10, cases 4 and 5 are implemented to show the impact of EVCS facilities on the grid operation performance. The uncontrolled case is where EVCS facilities are installed on arbitrary buses, and charging is not coordinated using a control strategy; hence the case shows a high power loss, severely disrupting grid performance.

A second implementation is developed to explore the benefit of the simultaneous planning mechanism, finding a less complex framework, discussed in Section 4.3. Like the preceding section, the section analyses the optimizer's strength in both the single and multi-objective optimization framework.

5.5.1. Single objective analysis

To further understand the efficiency of our proposed optimization scheme, we carry out a convergence test using the utility values from the IEEE 15-bus distribution network, shown in Fig. 11. It is observed from Fig. 11 that both proposed algorithms performs better than the benchmark algorithms. The effect of the EVCS implementation is also seen in Case 3 where the dynamic nature of the CoSGADE-I shows the fluctuation of utility values. The fluctuations are caused by the changes in grid performance after allocating EV charging stations at each iteration, meaning that the EVCS facilities can deter the planning solutions

Table 5
Unit allocation variables for the IEEE 118-bus distribution network.

Case	Optimizer	DG Allocation *Location(size(KW))*	BESS Allocation *Location(size(KW))*	CB Allocation *Location(size(KW))*	EVCS Allocation	% PL	VS	VD
III	GA	10(751.29), 35(792.84), 68(799.02), 90(879.71), 105(891.50), 113(778.34)	46(579), 80(650.59), 105(809.05), 113(799.89)	21(457), 45(736), 105(666), 69(733)	3, 9, 25, 47, 58, 84, 96, 115	13.6	0.0442	0.9203
	PSO	10(746.24), 34(794.07), 68(783.12), 95(883.72), 105(897.62), 113(779.18)	46(583.88), 83(682.83), 106(811.39), 113(784.27)	30(505), 44(581), 65(622), 105(587)	4, 11, 24, 42, 51, 78, 91, 105	13.5	0.0410	0.9221
	PSOGA	10(771.31), 33(798.04), 69(827.41), 86(882.11), 105(897.63), 116(772.92)	33(692), 81(589.43), 102(629.45), 117(554.02)	21(627), 45(730), 105(566), 69(705)	3, 9, 22, 47, 58, 84, 95, 115	29.4	0.0382	0.9310
	WOAGA	15(788.11), 38(792.74), 69(885.81), 85(889.59), 103(898.04), 117(789.59)	26(698.95), 83(595.58), 96(643.21), 117(561.72)	21(688), 45(771), 105(575), 69(719)	3, 9, 24, 47, 58, 84, 95, 115	29.8	0.0372	0.9333
	CoSGADE	32(675.96), 109(562.22), 113(384.17), 74(899.79), 33(450.05), 79(1015.66)	111(409.61), 110(350.11), 97(578.68), 117(670.99)	28(676), 43(651), 50(700), 64(669)	3, 9, 24, 47, 58, 84, 95, 115	32.3	0.0233	0.9409

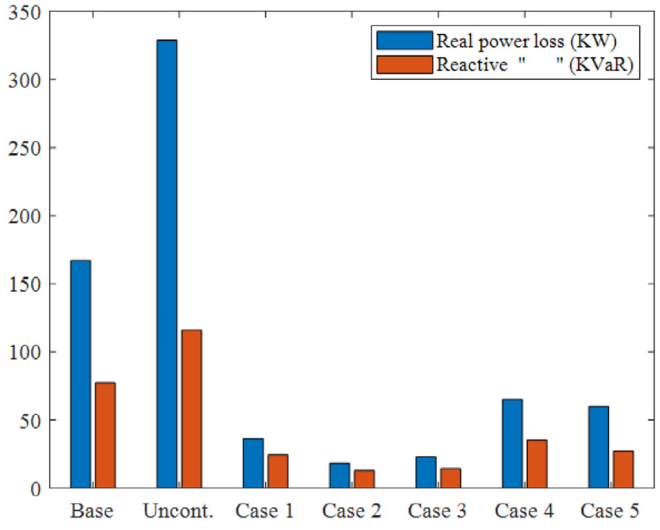

Fig. 9. Power loss profile of the 69-bus system for 5 case scenarios.

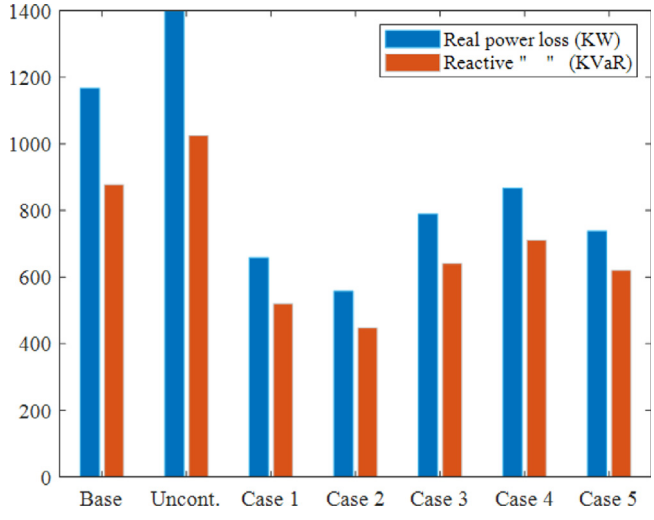

Fig. 10. Power loss profile of the 118-bus system for 5 case scenarios.

according to the next location of other DER or FACTS units. Also, we adopt the power loss minimization function to generate the convergence characteristic and computational complexity of each optimizer for the 69-bus and 118-bus distribution networks, shown in Figs. 12 and 13.

From Figs. 12 and 13, it is observed that the CoSGADE-I converges better than the other optimizers, including the CoSGADE-II. The CoSGADE-II follows a more practical evolutionary algorithm since all unit types are allocated at once for every iteration. Although less computationally complex, as seen from the computational time, its trade-off for optimality is marginally and relatively high. It is also observed that other optimizers use more computational time, given that the optimizers are not tailored for the proposed mechanism. Fig. 14 shows the boxplot that gives more insight into the performance of the algorithms. The boxplot is generated using solutions from 50 runs. The distribution of the solution is analysed, focusing on the variance to determine the consistency of each optimizer. It is seen from Fig. 14 that CoSGADE-I and II possess the smallest variance values, which can be determined by measuring the height of the box.

5.5.2. Multi-objective analysis

The performance of multi-objective optimizers is very important for practicality. In real-world scenarios, many objectives are

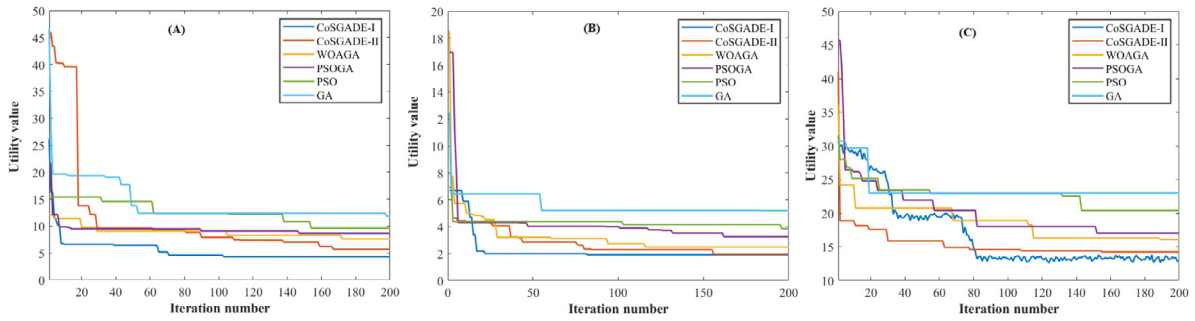

Fig. 11. Convergence plots of each algorithm for the IEEE 15-bus network. (A) PV and BESS unit allocation only, (B) PV, BESS, and CB allocation, and (C) PV, BESS, CB, and EVCS allocation.

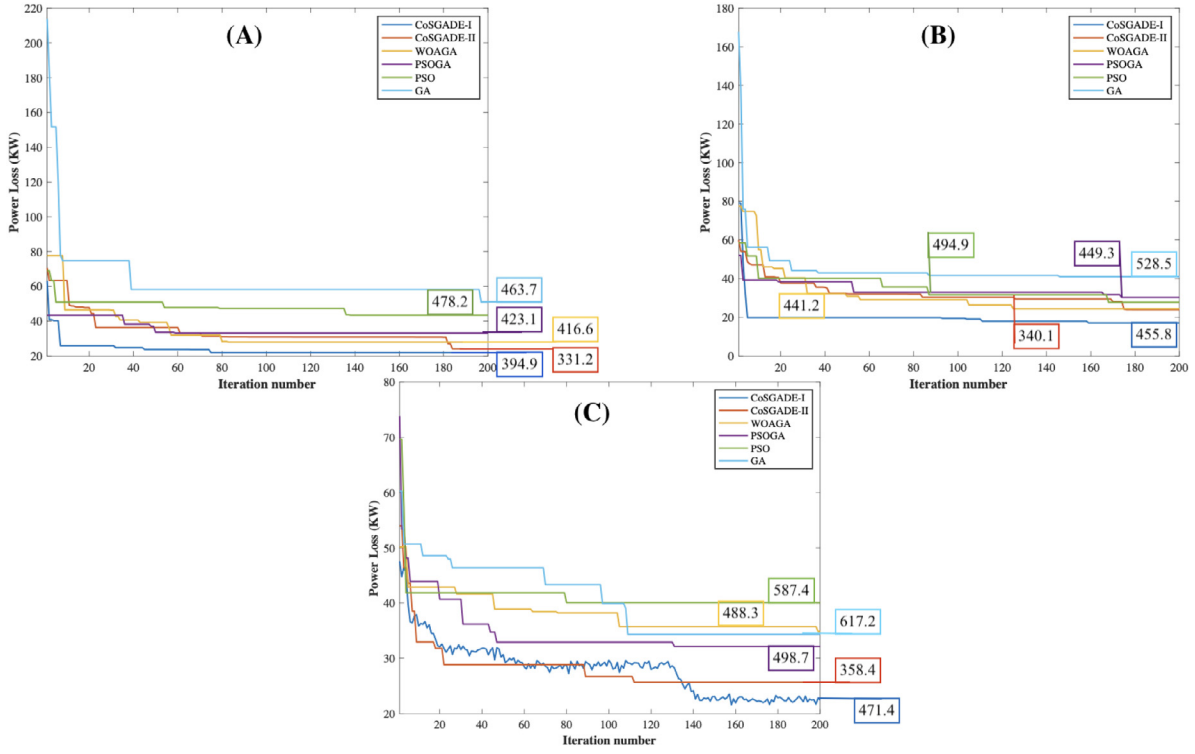

Fig. 12. Convergence and complexity analysis for the 69-bus system.

considered when planning a complex project like power system networks. This section provides information on the effect of the proposed optimizer via the proposed adaptive-dynamic planning mechanism in a multi-objective framework. The multi-objective form of the proposed optimizers, which are dubbed M-CoSGADE-I and II - Multi-objective CoSGADE, are formulated using the TOPSIS approach to generate optimal solutions. The MOO techniques are compared with other multi-objective optimizers. A spacing metric (SP-metric) is adopted for measuring the quality of solution distribution, determining the spread of all solutions and understanding the distribution. Table 6 shows the metrics for each multi-objective optimizer. It is observed that the proposed frameworks yield a better standard deviation score than other frameworks, interpreted as a compact solution distribution with good confidence in producing reliable, consistent results.

Table 6
Performance comparison of multi-objective optimization frameworks.

Technique	Mean	Best	Worst	Std. Dev.
MOPSO	0.062	0.065	0.081	0.015
NSGA-III	0.061	0.066	0.078	0.016
M-CoSGADE-II	0.053	0.054	0.063	0.012
M-CoSGADE-I	0.051	0.053	0.060	0.012

5.6. Validation of the adaptive-dynamic planning mechanism

To verify the efficacy of the proposed mechanism, we analyse its optimality and practicality on single and multi-objective optimization, comparing it with conventional planning mechanisms. Firstly, the CoSGADE optimizer is applied to all mechanisms to produce statistical parameters that determine the performance. Table 7 displays the statistical values for all mechanisms, showing a statistical measure of a 50-solution distribution for Case 3 of the 118-bus system, generated by the CoSGADE optimizer via different planning mechanisms.

It can be inferred from the table that the dynamic mechanism has a good standard deviation score, varying insignificantly from other schemes. It is to note that the main purpose of this analysis is to validate the correctness of the proposed planning mechanism, which passed successfully. The computational time

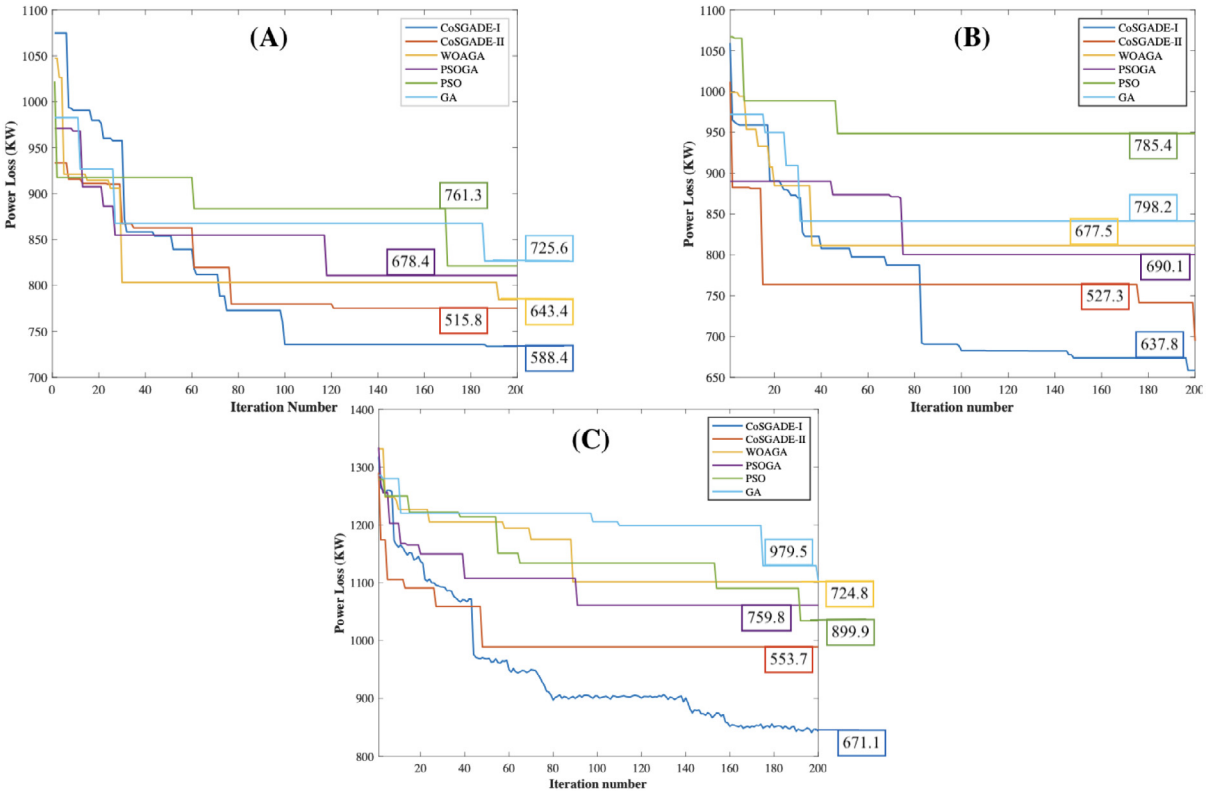

Fig. 13. Convergence and complexity analysis for the 118-bus system.

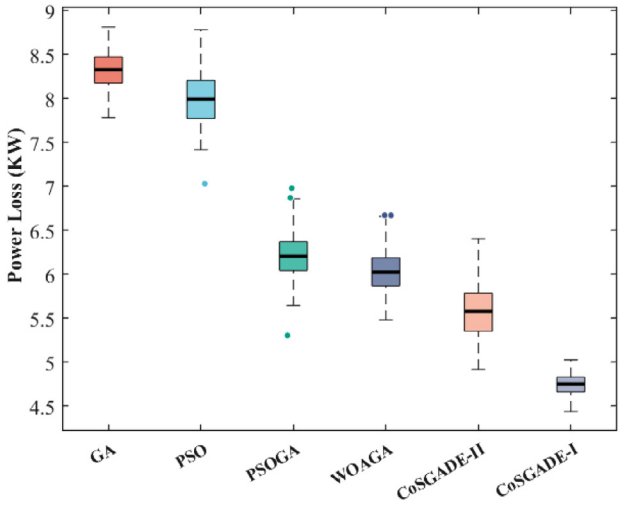

Fig. 14. Box plot analysis of each optimization scheme for the 15-bus system.

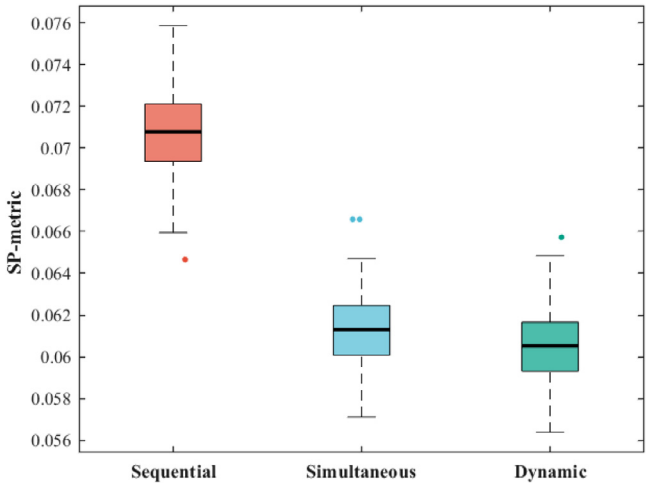

Fig. 15. Box plot analysis of each planning mechanism for the 118-bus system.

Table 7
Statistical comparison of the planning mechanisms.

Stat metric	Planning mechanisms		
	Sequential	Simultaneous	Dynamic
Best score	916.12	902.51	789.41
Worst score	931.45	930.67	806.62
Variance	0.41	0.26	0.23
Time (s)	253	126	369

is relatively fast when considering the multiple phases for every iteration.

Using 50 independent simulation runs, Fig. 15 illustrates the quality of solution distribution for each planning mechanism. It is seen that there is a strong similarity among all boxes, meaning that they have closely uniform distribution that a small variance and an efficient mechanism.

5.7. Further discussion

In this section, we discuss more on the numerical results from the simulation of the planning model. Attention is paid to the impact of the planning mechanism and the optimization scheme on different system scales, aiming at efficiency and optimality. Sampling the simulation results for each case, it is seen that the introduction of EVCS facilities deters the grid operation performance, even with an EV charging control strategy. Although still

improved by the CoSAGDE optimizer, it is important to know the significance of introducing such facilities to a distribution network. The introduction of capacitors reduces the negative effect, as seen in case 2 for all study systems. This effect is even more distinct in Section 5.5, where another case is introduced — allocating only PV-DG, BESS, and EVCS facilities. However, it is essential to note that capacitors are expensive and may not be practically viable. Bearing this in mind, another case; case 5, was introduced to inject reactive power from EV chargers into the grid network. As a result, relatively minimized real and reactive power losses can be seen in Figs. 9 and 10, hence improving grid performance.

Another observation is the performance of the optimizers on different study systems. The 15-bus and 69-bus systems clearly improve grid performance after implementing all cases, while the 118-bus has a less significant improvement. This effect shows the influence of a scaled problem on the algorithm performance and the manifesting of the No Free Lunch Theorem even for the same problem of different scales. Furthermore, Figs. 12 and 13 show a convergence curve that depicts the behaviour of the proposed CoSGADE-I, particularly for the 118-bus system, where the optimizer converges differently for different cases. It is seen that introducing EVCS facilities influence the complexity of the model, which results in the slow convergence of the CoSGADE-I. The slowness results from a systematic exploration and exploitation of the search space, which proves fruitful as it has a better power loss for its allocation variables.

Finally, the impact of evolutionary algorithms for discrete optimization is evident in the location variables. Remembering that the adopted benchmark hybrid algorithms — WOAGA and PSOGA are implemented using the same approach as the CoSGADE, where each algorithm solves different variable types, it is seen that the optimal location variables produced by all adopted algorithms are very similar. For example, the EVCS locations are the same for the 15-bus and 69-bus systems and vary slightly for the 118-bus system. The same is observed for the location of other unit types, with only the PSO algorithm producing dissimilar solutions.

6. Conclusion

In this paper, we investigated the impact of planning mechanisms on optimal allocation variables in smart grid planning frameworks. To this effect, we formulated a single- and multi-objective planning problem, considering power loss, voltage stability, and voltage deviation. After that, an adaptive-dynamic planning mechanism, which is an underlay for the optimization process, is proposed to generate optimal solutions. The planning mechanism, formed using a recombination technique, showed an expanded solution space, validated using two-, three-, and four-unit type allocation schemes for both single- and multi-objective optimization frameworks on 15-bus, 69-bus, and 118-bus distribution networks. The numerical simulations demonstrate a good variance in the distribution of optimal allocation variables but come with relatively higher complexity when compared to conventional planning mechanisms. To address this challenge, two implementations of the proposed CoSGADE is developed, which reduce the complexity (adopting computational time) and also improve grid performance.

Future work will research on reducing the complexity of the planning mechanism. Focus will also be on the addition of more unit types and constraints to observe the increase in complexity.

CRediT authorship contribution statement

Kayode E. Adetunji: Conceptualization, Software, Formal analysis, Data curation, Validation, Visualization, Writing – original draft. **Ivan W. Hofsajer:** Supervision, Resources, Writing – review & editing. **Adnan M. Abu-Mahfouz:** Supervision, Resources, Funding acquisition, Writing – review & editing. **Ling Cheng:** Methodology, Formal analysis, Supervision, Funding acquisition, Writing – review & editing.

Declaration of competing interest

The authors declare that they have no known competing financial interests or personal relationships that could have appeared to influence the work reported in this paper.

Data availability

Data will be made available on request.

References

Abdel-Mawgoud, H., Kamel, S., Khasanov, M., Khurshaid, T., 2021. A strategy for PV and BESS allocation considering uncertainty based on a modified Henry gas solubility optimizer. Electr. Power Syst. Res. 191, 106886.
Abou El-Ela, A.A., El-Seheimy, R.A., Shaheen, A.M., Wahbi, W.A., Mouwafi, M.T., 2021. PV and battery energy storage integration in distribution networks using equilibrium algorithm. J. Energy Storage 42, 103041.
Adetunji, K.E., Hofsajer, I.W., Abu-Mahfouz, A.M., Cheng, L., 2021. Category-based multiobjective approach for optimal integration of distributed generation and energy storage systems in distribution networks. IEEE Access 9, 28237–28250.
Adetunji, K.E., Hofsajer, I.W., Abu-Mahfouz, A.M., Cheng, L., 2022. An optimization planning framework for allocating multiple distributed energy resources and electric vehicle charging stations in distribution networks. Appl. Energy 322, 119513.
Awad, A.S., El-Fouly, T.H., Salama, M.M., 2015. Optimal ESS allocation for load management application. IEEE Trans. Power Syst. 30 (1), 327–336.
Barukčić, M., Varga, T., Jerković Štil, V., Benšić, T., 2021. Co-simulation framework for optimal allocation and power management of DGs in power distribution networks based on computational intelligence techniques. Electronics 10 (14), 1648.
Biswal, S.R., Shankar, G., Elavarasan, R.M., Mihet-Popa, L., 2021. Optimal allocation/sizing of DGs/capacitors in reconfigured radial distribution system using quasi-reflected slime mould algorithm. IEEE Access 9, 125658–125677.
Bozorgavari, S.A., Aghaei, J., Pirouzi, S., Vahidinasab, V., Farahmand, H., Korpås, M., 2019. Two-stage hybrid stochastic/robust optimal coordination of distributed battery storage planning and flexible energy management in smart distribution network. J. Energy Storage 26, 100970.
Das, C.K., Bass, O., Kothapalli, G., Mahmoud, T.S., Habibi, D., 2018. Overview of energy storage systems in distribution networks: Placement, sizing, operation, and power quality. Renew. Sustain. Energy Rev. 91 (March), 1205–1230.
Das, C.K., Bass, O., Mahmoud, T.S., Kothapalli, G., Masoum, M.A., Mousavi, N., 2019. An optimal allocation and sizing strategy of distributed energy storage systems to improve performance of distribution networks. J. Energy Storage 26 (June), 100847.
Das, S., Suganthan, P.N., 2011. Differential evolution: A survey of the state-of-the-art. IEEE Trans. Evol. Comput. 15 (1), 4–31.
Erdinc, O., Tascikaraoglu, A., Paterakis, N.G., Dursun, I., Sinim, M.C., Catalao, J.P., 2018. Comprehensive optimization model for sizing and siting of DG units, EV charging stations, and energy storage systems. IEEE Trans. Smart Grid 9 (4), 3871–3882.
Fang, W., Zhu, H., Mei, Y., 2022. Hybrid meta-heuristics for the unrelated parallel machine scheduling problem with setup times. Knowl.-Based Syst. 108193.
Gampa, S.R., Jasthi, K., Goli, P., Das, D., Bansal, R.C., 2020. Grasshopper optimization algorithm based two stage fuzzy multiobjective approach for optimum sizing and placement of distributed generations, shunt capacitors and electric vehicle charging stations. J. Energy Storage 27 (November 2019), 101117.
Islam, S.M., Das, S., Ghosh, S., Roy, S., Suganthan, P.N., 2012. An adaptive differential evolution algorithm with novel mutation and crossover strategies for global numerical optimization. IEEE Trans. Syst. Man Cybern. B 42 (2), 482–500.
Janamala, V., Reddy, D.S., 2021. Coyote optimization algorithm for optimal allocation of interline–photovoltaic battery storage system in islanded electrical distribution network considering EV load penetration. J. Energy Storage 41, 102981.

Jeddi, B., Vahidinasab, V., Ramezanpour, P., Aghaei, J., Shafie-khah, M., Catalão, J.P., 2019. Robust optimization framework for dynamic distributed energy resources planning in distribution networks. Int. J. Electr. Power Energy Syst. 110 (February 2018), 419–433.

Kansal, S., Kumar, V., Tyagi, B., 2013. Optimal placement of different type of DG sources in distribution networks. Int. J. Electr. Power Energy Syst. 53 (1), 752–760.

Kaur, K., Kumar, N., Singh, M., 2019. Coordinated power control of electric vehicles for grid frequency support: MILP-based hierarchical control design. IEEE Trans. Smart Grid.

Mirjalili, S., Lewis, A., 2016. The whale optimization algorithm. Adv. Eng. Softw. 95, 51–67.

Mouwafi, M.T., El-Sehiemy, R.A., Abou El-Ela, A.A., 2021. A two-stage method for optimal placement of distributed generation units and capacitors in distribution systems. Appl. Energy 118188.

Mukhopadhyay, B., Das, D., 2020. Multi-objective dynamic and static reconfiguration with optimized allocation of PV-DG and battery energy storage system. Renew. Sustain. Energy Rev. 124 (February), 109777.

Paliwal, P., Patidar, N.P., Nema, R.K., 2014. Planning of grid integrated distributed generators: A review of technology, objectives and techniques. Renew. Sustain. Energy Rev. 40, 557–570.

Pereira, L.D., Yahyaoui, I., Fiorotti, R., de Menezes, L.S., Fardin, J.F., Rocha, H.R., Tadeo, F., 2022. Optimal allocation of distributed generation and capacitor banks using probabilistic generation models with correlations. Appl. Energy 307, 118097.

Pirouzi, S., Zaghian, M., Aghaei, J., Chabok, H., Abbasi, M., Norouzi, M., Shafie-khah, M., Catalão, J.P., 2022. Hybrid planning of distributed generation and distribution automation to improve reliability and operation indices. Int. J. Electr. Power Energy Syst. 135, 107540.

Rodríguez-Gallegos, C.D., Yang, D., Gandhi, O., Bieri, M., Reindl, T., Panda, S.K., 2018. A multi-objective and robust optimization approach for sizing and placement of PV and batteries in off-grid systems fully operated by diesel generators: An Indonesian case study. Energy 160, 410–429.

Salama, M.M., Chikhani, A.Y., 1993. A simplified network approach to the var control problem for radial distribution systems. IEEE Trans. Power Deliv. 8 (3), 1529–1535.

Schweppe, F.C., Wildes, J., 1970. Power system static-state estimation, Part I: Exact model. IEEE Trans. Power Appar. Syst. PAS-89 (1), 120–125.

Shaheen, A.M., El-Sehiemy, R.A., 2020. Optimal co-ordinated allocation of distributed generation units/ capacitor banks/ voltage regulators by EGWA. IEEE Syst. J. 1–8.

Singh, P., Bishnoi, S.K., Meena, N.K., 2020a. Moth search optimization for optimal DERs integration in conjunction to OLTC tap operations in distribution systems. IEEE Syst. J. 14 (1), 880–888.

Singh, P., Bishnoi, S.K., Meena, N.K., 2020b. Moth search optimization for optimal DERs integration in conjunction to OLTC tap operations in distribution systems. IEEE Syst. J. 14 (1), 880–888.

Thokar, R.A., Gupta, N., Niazi, K., Swarnkar, A., Meena, N.K., 2021. Multiobjective nested optimization framework for simultaneous integration of multiple photovoltaic and battery energy storage systems in distribution networks. J. Energy Storage 35, 102263.

Uddin, M., Romlie, M.F., Abdullah, M.F., Abd Halim, S., Abu Bakar, A.H., Chia Kwang, T., 2018. A review on peak load shaving strategies. Renew. Sustain. Energy Rev. 82 (October 2017), 3323–3332.

Wong, L.A., Ramachandaramurthy, V.K., Walker, S.L., Taylor, P., Sanjari, M.J., 2019. Optimal placement and sizing of battery energy storage system for losses reduction using whale optimization algorithm. J. Energy Storage 26 (July), 100892.

Yang, Y., Li, H., Aichhorn, A., Zheng, J., Greenleaf, M., 2014. Sizing strategy of distributed battery storage system with high penetration of photovoltaic for voltage regulation and peak load shaving. IEEE Trans. Smart Grid 5 (2), 982–991.

Zheng, Y., Niu, S., Shang, Y., Shao, Z., Jian, L., 2019. Integrating plug-in electric vehicles into power grids: A comprehensive review on power interaction mode, scheduling methodology and mathematical foundation. Renew. Sustain. Energy Rev. 112 (June), 424–439.